# Exploring the effects of platinum compounds on RNA, adduct formation, thermal melting properties and siRNA down regulation capacity of gene targets associated with cancer

**Name: Alak Alshiekh**

Department of Biochemistry and Structural Biology-Protein science master program

Master thesis 60 credits: January 2011-December 2011

**Supervisors: Christopher Polonyi, Hanna Hedman**

**Examiner: Sofi Elmroth**

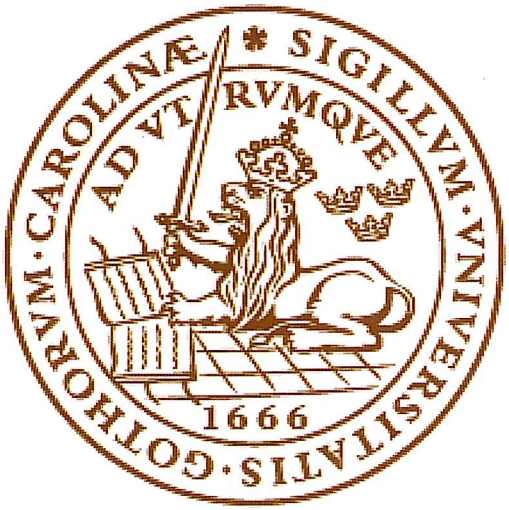


LUNDS UNIVERSITET

Naturvetenskapliga fakulteten

*Alak ALshiekh*

## Undersökning utav effekten av platinaföreningar på RNAi, adduktformation, smältpunkt och förmågan hos siRNA att nedreglera gener associerade med cancer

DNA och RNA är nukleinsyror. DNA är bärare av den genetiska koden som översätts till RNA och senare till proteiner. Proteiner är den typ av molekyler som gör grovjobbet i cellen.

RNA interference (RNAi) är en naturligt fenomen. Det betyder att små fraktioner av dubbelsträngat RNA kontrollerar hur mycket proteiner som skall produceras. Det finns olika typer av RNAi-molekyler, t.ex. micro RNA som är producerat i cellen och s.k. siRNA som kan introduceras i cellen.

Cancer är en genetiskt orsakad sjukdom. Det finns bra behandlingar för många typer av cancer. Cisplatin och oxaliplatin är vanligt använda metallbaserade läkemedel. Cisplatin och oxaliplatin påverkar nukleinsyror, genom att direkt reagera med olika kemiska grupper. Försök är på gång där RNAi användas som en behandling för sjukdomar av den här typen.

I det här projektet, försöker vi att ta reda på vad som händer när RNAi och platina behandlingen arbetar tillsammans i en cancercell. Vi har testat hur platina påverkar RNAi, både när RNA molekyler exponerats för platina i förväg, och även efter det att de tagits upp i cellen. Vi har försökt att ta reda på hur platina ändrar stabiliteten av siRNA, eftersom stabiliteten är mycket viktigt för funktion.

BRCA1 och Wnt5a är proteiner som är mycket viktiga i cancerprocessen. Vi har använt siRNA sekvenser som stör produktionen av BRCA1 och Wnt5a och undersökt hur dessa sekvenser kan modifiera produktionen av BRCA1 och WNt5a. Hur det platinerade siRNAt påverkar funktionen i cancercellerna har också undersökts.

Handledare: **Christopher.Polonyi, Hanna Hedman**
Examensarbete 60 hp i Januari-december.* 2011
Kemicentrum, Lunds universitet
Av. Biokemi och strukturbiologi

*Examensarbetsämne: Proteinvetenskap: Examensarbete för masterexamen.

# Abstract

Since its discovery, RNA interference (RNAi) has turned into an invaluable research tool for regulating gene expression. Furthermore, this naturally occurring phenomenon in mammalian cells is of interest in cancer research, both as a possible therapeutic approach and a target for cancer treatment. Platinum anticancer agents like cisplatin are considered one of the most active cancer drugs used either alone or in combination therapy. Cisplatin has made its way from the accidental discovery in 1965 to the first patient treated in 1971. The validated target of platinum cancer treatment is DNA. Other targets include RNA and protein. In this work, the aim was to shed more light on the interaction between platinum based drugs and RNA, investigating the interaction with double stranded RNAs that are 20 nucleotides in length. The effect of platination on RNA thermodynamic stability and function in a cellular environment was studied. Further knowledge in this area will be helpful in developing siRNA-based therapies, and to elucidate possible interactions that might arise from the combination of platinum based treatments and small interfering RNA (siRNA) based therapeutics e.g. the possibility of synergistic effects. Endogenous miRNA play a major role in the cancerous cell environment. A closer look at the interplay between platinum-based treatment and oncomiRs could be verified as additional therapeutic targets of platinum drugs. Several synthetic siRNA sequences that were designed to target regions of 3'-UTR of the proteins BRCA1 and Wnt5a were studied in the present work, both proteins have a strong association with human cancers. The chosen sequences were evaluated by thermal melting studies and platination reactions. Purification of platination products was performed to investigate the effects of cisplatin and oxaliplatin on both duplex stability and down regulating capacity in a cellular environment. siRNAs were studied by denaturing poly acrylamide gel electrophoresis (PAGE).

The down regulating ability was investigated in a cellular system consisting of MCF-7 breast cancer cells by using two model protein systems. The effect of siRNA on endogenous BRCA1 protein levels was evaluated by Western blot. The effect of platination on siRNA's downregulation capacity was investigated by Luciferase assays with Wnt5a 3'-UTR as atarget. Purified platination products or native siRNAs were transfected into MCF-7 cells and

comparison of luciferase production by luminometry was measured. Introduction of oxaliplatin in concentrations below previously determined $IC_{50}$ values in MCF-7 cell lines after transfection of unplatinated siRNAs served to evaluate the effect on down regulation capacity.

# Contents

List of abbreviations ..... 9

1-Introduction ..... 11

1-1 Cancer ..... 11

1-2 Platinum anticancer drugs ..... 11

1-3 Nucleic acids ..... 13

1-4 RNA interference ..... 13

1-5 miRNAs and cancer ..... 14

1-6 RNA interference and its potential in therapeutic applications ..... 15

1-7 BRCA1 ..... 15

1-8 Wnt5a ..... 15

2-Aim ..... 16

3-Materials and methods ..... 17

3-1 Nucleic acid sequences and plasmids used ..... 17

3-2 Cell lines and cell culture techniques ..... 17

3-3 Transfection ..... 19

3-4 BCA protein determination ..... 19

3-5 BRCA1 downregulation ..... 19

3-6 Cell lysis ..... 19

3-7 Luminescence measurements and normalization ..... 20

3-8 SDS-PAGE ..... 20

3-9 Western blot ..... 20

3-10 MTT assay ..... 20

3-11 Purification of nucleic acids by gel electrophoresis and UV shadowing ..... 21

3-12 Ethanol precipitation ..... 21

3-13 Nucleic acid concentration determination ..... 21

3-14 Oxaliplatin's effect on siRNA efficacy in MCF-7 cells ..... 22

3-15 Platination of siRNAs ..... 22

3-16 Digestion of nucleic acids ..... 22

3-17 Radiolabeling, gel purification and precipitation of oligonucleotides ..... 22

3-18 Thermal melting analysis and van't Hoff's plot ..... 23

3-19 Screening the miRNA database (miRBase) for human miRNAs with possible platination sites ..... 23

3-20 Effect of platination on silencing ability of W- siRNA -101 ..... 23
4-Results and discussion ..... 25
4-1 MTT cell survival assay ..... 25
4-2 Effects of oxaliplatin on siRNA efficacy in MCF-7 cells ..... 26
4-3 BRCA1 level detection by Western blotting ..... 27
4-4 BRCA1 downregulation with siRNA ..... 28
4-5 Sequencing of the antisense strand of W- siRNA -139 and determination of platination sites ..... 28
4-6 Screening the miRNA database (miRBase) for human miRNAs with possible platination sites ..... 29
4-7 RNaseA working range determination ..... 30
4-8 Effect of platination on silencing ability of W- siRNA -101 ..... 33
4-9 Thermal melting studies of W-siRNA-139 and van't Hoff plot analysis ..... 35
4-10 Platination effect on melting temperature (Tm) and thermodynamic parameters ..... 37
5-Conclusions ..... 41
6-Future perspectives ..... 41
7-Acknowledgments ..... 41
8-References ..... 42
9-Appendix ..... 43
9-1List of Figures ..... 43
9-2 Table legends ..... 45
9-3 3'UTR sequences ..... 46

## List of abbreviations

| | |
|---|---|
| A | adenine |
| BCA | bicinchoninic acid assay |
| C | cytosine |
| Cisplatin | cis-Pt: *cis*-diamine dichloride platinum |
| CPS | counts per second |
| DACH | diaminecyclohexane |
| DDT | dichlorodiphenyltrichloroethane |
| DMEM | Dulbecco's modified Eagle's medium |
| DMSO | dimethylsufoxide |
| ds | double stranded |
| G | guanine |
| HRP | horse radish peroxidase |
| miRNA | micro RNA |
| MMR | mismatch repair |
| NaOAc | sodium acetate |
| NER | nucleotide excision repair |
| Oxaliplatin | *SP*-4-2-(*1R-trans*)]-(1,2-cyclohexanediamine-N,N)[ethandioata-O,O]platinum(II) |
| PAGE | polyacrylamide gel electrophoresis |
| Pt | platinum |
| PTGS | post transcriptional gene silencing |
| RISC | RNA induced silencing complex |
| RNAi | RNA interference |
| SDS | sodium dodecylsulfate |
| siRNA | small interfering RNA |

| | |
|---|---|
| ss | single stranded |
| T4PNK | T4 polynucleotide kinase |
| Tm | melting temperature |
| U | uracil |
| UTR | untranslated region |
| w-siRNA-101 | siRNA targeting from basepare 101 of 3'-UTR of Wnt5a protein |
| W-siRNA-101 cisPt 1-1 | contains one cisPt adducts 1st purification batch |
| W-siRNA-101 cisPt 1-2 | contains one cisPt adducts 2nd purification batch |
| W-siRNA-101 cisPt2-1 | contains two cisPt adducts 1st purification batch |
| W-siRNA-101 cisPt2-2 | contains two cisPt adducts 2nd purification batch |
| W-siRNA-101 oxPt 1-1 | contains one oxPt adducts 1st purification batch |
| W-siRNA-101 oxPt 1-2 | contains one oxPt adducts 2nd purification batch |
| W-siRNA-101 oxPt 2-1 | contains two oxPt adducts 1st purification batch |
| W-siRNA-101 oxPt 2-1 | contains two oxPt adducts 2nd purification batch |
| w-siRNA-139 | siRNA targeting from basepare 139 of 3'-UTR of Wnt5a protein |
| w-siRNA-147 | siRNA targeting from basepare 147 of 3'-UTR of Wnt5a protein |
| w-siRNA-33 | siRNA targeting from basepare 33 of 3'-UTR of Wnt5a protein |

# 1-Introduction

## 1-1 Cancer

Cancer is a class of diseases that involves dynamic changes in the genome by mutations that produce increasingly potent oncogenes and less functioning tumor suppressor genes. Tumorigenesis in humans is a multistep process of genetic alterations driving normal cells to turn into malignant ones. Cancer cells are defect in their regulatory circuits in particular thosethat govern cell proliferation and homeostasis. The physiological changes that give cancer cells the ability to evade anticancer defense mechanisms are believed to be shared by most human cancers, such as their self sufficiency in growth signals, insensitivity to growth inhibitory signals, evading apoptosis, unlimited replication potential, sustained angiogenesis and tissue invasion and metastasis.[1]

## 1-2 Platinum anticancer drugs

Platinum based drugs are clinicaly used anti-cancer agents and are used for a variety of malignancies. Lately, efforts have been made to synthesize analogues with an enhanced activity spectrum, reduced toxicity or to overcome cellular resistance.[2] How these compounds came to this clinical use is a serendipitous rediscovery of a previously synthesized compound by Michele Peyrone in 1844 that took an interesting twist.

In the 1960s, Rosenberg et al. discovered cisplatin (see Figure 1) while investigating the effect of electric fields on bacterial growth. He grew *E.coli in* an aerobic solution containing $NH_4Cl$ and used platinum electrodes. The bacteria grew 300 times their normal length and did not divide in a normal manner.[3]

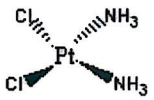


**Figure 1** Cisplatin, *cis*-Pt *Cis*-diamine dichloride platinum (II).

Rosenberg and coworkers chose platinum electrodes assuming chemical inertness, and applied an 1000 c/s electric field assuming elimination of electrolysis effects and electrode polarization. After applying the voltage they observed a cessation in bacterial growth and the formation of long filaments with rapidly increasing length. The length increase continued after removal of the voltage with an observed morphological change under the phase contrast microscope. They established that an oxidizing chemical species created by an electric current caused the elongation of the bacteria. Their tests established that a concentration of 10 p.p.m. of $(NH_4)_2PtCl_6$ for more than 2 hours caused the appearance of filaments.[4]

Cisplatin is activated intracellularly by aquation of one of the two chloride leaving groups and subsequently binds to DNA, forming DNA adducts. Later on, various signal transduction

pathways get activated, for example, pathways involved in cell-cycle arrest, apoptosis and DNA--damage recognition.[5] The aquated species of cisplatin is the reactive form of the compound that binds nucleophilic groups containing oxygen, nitrogen, or sulphur atoms which are abundant in amino acids, RNA and DNA. The rate limiting step is the formation of the monoaqua species. The majority of DNA platinum adducts are 1,2-GpG or 1,2-ApG intrastrand crosslinks. The formation of GG adducts introduces a strong kink in the structure. Cisplatin adducts are repaired by the nucleotide excision repair (NER) machinery with poor efficiency, because they are bound to high mobility group proteins. These adducts block elongation by transcribing polymerases and trigger apoptosis. Thus, the inability of the cells to repair those adducts contribute to the efficacy of cisplatin.[6]

*SP*-4-2-(1*R-trans*)]-(1,2-cyclohexanediamine-*N,N*)[ethandioata-*O,O*]platinum(II) or oxaliplatin (see Figure 2) is a platinum cancer drug with a different spectrum of activity, mechanism of action and resistance when compared to cisplatin. Diaminocyclohexane (DACH) containing compounds have shown antitumor activity in cells resistant to cisplatin such as in colorectal cancer where cisplatin showed no activity in increasing patient survival and oxaliplatin showed potent cytotoxic activity.

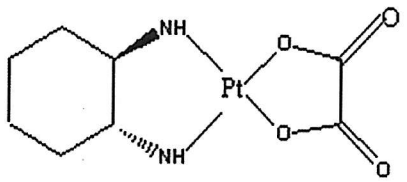


**Figure 2.** Oxaliplatin, *SP*-4-2-(1*R-trans)*]-(1,2-cyclohexanediamine-*N,N*)[ethandioata-*O,O*]platinum(II).

*In vivo* studies showed oxaliplatin activity against breast, colon and gastric cancer, renal cell carcinoma and sarcoma. The current central paradigm in the field is that platinum compounds exert their cytotoxic effect by causing DNA damage. Even though oxaliplatin is more cytotoxic than cisplatin, it shows lower reactivity than cisplatin with naked DNA. Furthermore, experiments show fewer DNA adducts when compared with cisplatin at equimolar and/or equitoxic concentrations, finally, the proportion of DNA single-strand breaks are remarkably higher with oxaliplatin compared to cisplatin. The lower levels of platinum adducts formed are most likely reflecting the slow dissociation rate of the oxalate ligand under physiological conditions. The DACH ligand might induce DNA lesions that are poorly recognized by repair pathways. Even though adducts are similar in structure, the bulkier DACH moiety that protrudes into the minor groove appears to have different biological properties. Oxaliplatin was noted to have equivalent cytotoxicity to cisplatin even though it causes fewer DNA platinum adducts. Cellular resistance against cisplatin can be attributed to decreased accumulation, increased deactivation by glutatione or increased tolerance to Pt-DNA adducts. In the first two cases of

resistance mechanisms cells show similar resistance to oxaliplatin. The potential differences between cisplatin and oxaliplatin may arise from cells ability to repair Pt-DNA adducts by NER, mismatch repair (MMR), downstream responses contributing to distinct cell death mechanism and postreplicative mechanisms e.g. DNA chain elongation and replicative bypass.[5]

## 1-3 Nucleic acids

Nucleic acids are remarkable molecules that represent the reservoir of genetic information. They are polymeric chains in which the monomer units are connected by covalent bonds. The monomer units contain a five carbon sugar which corresponds to ribose in RNA and deoxyribose in DNA. These moieties are connected to eachother via a phosphodiester link between two sugar residues. Each monomer carries a heterocyclic base at the 1' C of the sugar residue and these bases are either purines; adenine (A) and guanine (G), or pyrimidines; cytosine (C) and thymine (T) (in DNA) or uracil (U) (in RNA). An individual molecular strand of nucleic acids can specifically pair with a second strand, forming a double strand because of the intrinsic base pairing capability of the nucleotide bases. This characteristic attribute is very important in biology, since both the stability [7] of the double strand structure and the possibility of strand separation is very critical. Enthalpic contributions ($\Delta H$) come from hydrogen bonds between base pairs and Van der Waals interactions between stacked bases. Energy must be spent to break the bonds and the interactions. At low temperature the entropic contributions ($\Delta S$) will be lower than the enthalpic contribution ($\Delta H$) and the duplex is more stable. As temperature increases double stranded structure becomes unstable and denatures. At the melting temperature ($T_m$) the denatured (single stranded, ss) fraction is equal to the native (double stranded, ds) fraction.[8]

## 1-4 RNA interference

RNA interference (RNAi) is a gene silencing mechanisim triggered by double stranded (ds) RNA. This potent and specific phenomenon was reported in *Caenorhabtidis elegans* described by Andrew Fire and Craig Mello in their letter to nature [9] In this pioneering study either purified sense or antisense single stranded or preannealed double stranded RNA sequences that cover a 742 nucleotide segment of the *unc-22* gene were introduced in the worm *C.elegans.* Downregulation of this gene leads to an observable twitching phenotype in *C.elegans*. Contrary to their expectations, the double stranded RNA was evidently more potent at producing interference than either of the single strands alone. Fire and Mello observed an evident interference in both the injected animals and their progeny, and the effect could also spread from tissue to tissue. The interference by ds RNA was described to be very specific, and only exerted effect when the dsRNA sequence was homologous to the target gene.[9] This remarkable observation that led to Fire and Mello receiving the Nobel prize in physiology or medicine in 2006, required a hypotheses calling for a paradigm shift. Prior to this report, dsRNA was presumed to be a nonspecific silencing agent triggering the destruction of mRNA. Furthermore, the energetic stability of dsRNA and its incapability of further specific Watson-Crick base pairing demanded the investigation of cellular mechanisms to introduce RNA unwinding and

promote further search for a complementary sequence. Fire's suggestion, that dsRNA is the trigger for RNAi in *C.elegance,* lead to the comparison of RNAi with posttranscriptional gene silencing (PTGS), co-suppression and quelling which were observed in other organisms. This comparison suggested a common underlying mechanism.[10] This widespread natural phenomenon observed in fungi, plants and animals turned into a powerful genetic tool for initiation of gene silencing. RNAi can be triggered by various RNA molecule sources such as RNA viruses, transposons, siRNAs which are exogenous (~21 nucleotide dsRNA) or endogenous miRNAs (~19-25 nucleotide long) that have an important role in cellular function.

Long dsRNAs get converted to 21-23 nucleotides siRNAs by Dicer, which is an RNase III-type enzyme that yields products with two nucleotide 3'overhangs and phosphate groups at the 5'-end. Both linear and hairpin RNA structures can be processed by Dicer. siRNA sequences have sense and antisense strands in respect of their target mRNA. The antisense strand (also denoted the guide strand) serves as the template for the sequence specific gene silencing. The sense strand (also called is the passenger strand) gets degraded. Following the assembly of siRNA with the RNA-induced silencing complex (RISC), the siRNA-RISC complex will bind the target mRNA and cleavage is induced between nucleotide 10 and 11 upstream of the 5'end of the guide strand. The target mRNA is cleaved and degraded when complementarity between the guide and the target strand is perfect.

miRNA biogenesis takes place in the cell nucleus, where miRNAs are transcribed by RNA polymerase II forming pri-miRNA containing a 5'-cap and poly-A tail sequence. The protein complex Drosha-DGCR8 crops these stem looped pri-miRNAs yielding 70 nucleotide pre-miRNAs. Drosha, a nuclear RNase III, interacts with Pasha (DGCR8) and yields RNA products containing 5' phosphate groups and two nucleotide overhangs. Pasha and Drosha specifically recognize and bind the pri-miRNA and this interaction is dependent on the flanking ssRNA in the pri-miRNA. The ruler for Drosha cleavage is determined at ~11 base pairs from the stem-ssRNA junction by the Pasha-RNA interaction. Pre-miRNA have to be transported to the cytoplasm by the exportin-5 RanGTP transport receptor complex. The pre-miRNA gets released from the complex in the cytoplasm by the hydrolysis of GTP, followed by Dicer processing into mature miRNAs ~22 nucleotides in length that get loaded onto the RISC complex. The imperfect matching between the 3'-UTR target and the miRNA will not lead to target cleavage, but to repression of translation.[11]

## 1-5 miRNAs and cancer

The first evidence of miRNA involvement in cancer, was the finding that *miR-15a* and *miR-16-1* are down-regulated or deleted in most chronic lymphocytic leukemia (CLL).[12] These miRNAs are located in an intron of a gene that is deleted in 65% of all CLL cases, 50% of mantle-cell lymphomas, 10-40% of multiple myelomas and 60% of prostate cancer cases. Further investigation revealed that 50% of the known miRNAs are located inside or close to fragile sites and common breakpoints associated with cancer. miRNAs are differently expressed in tumors

compared to normal tissue. Theses differences are tumor specific, and could be associated with prognosis in some cases. There is a unique miRNA signature (consists of 42 miRNAs) that distinguishes tumor from normal tissue. A miRNA that targets an oncogene could be considered a tuomore suppressor and it could be downregulated in some cancers whereas a miRNA that targets a tumor suppressor might be considered an oncogene and it can be upregulated in some cancers [12].

## 1-6 RNA interference and its potential in therapeutic applications

RNAi based therapeutics has the potential to be a powerful tool for specific and potent inhibition of therapeutic targets of different molecular classes. RNAi has the advantage of targeting specifically and potently even nondruggable targets. One advantage with the RNAi strategy is that both the identification of highly selective sequences and the synthesis of these sequences are rapid processes. Finding successful clinically applicable delivery strategies remains the major challenge for RNAi based drug development. Other obstacles to overcome are stability against nuclease degradation and avoiding off-target effects and several chemical modifications are being investigated in order to overcome these obstacles [13] and today a handful of candidates are already undergoing clinical trials.

## 1-7 BRCA1

The breast cancer susceptibility gene (BRCA1) is a tumor suppressor gene located on chromosome 17q12-21 that has been thoroughly investigated since its identification and cloning of BRCA1 gene in 1994 on by Miki et al. BRCA1 hereditary mutations account for 40-45% of hereditary breast cancers and its expression is frequently reduced or absent in sporadic cancers. Among other functions, BRCA1 plays a role in cell cycle progression, DNA repair processes, cell cycle check points that are DNA damage responsive and apoptosis.[14]

## 1-8 Wnt5a

Wnt5a belongs to a family of secreted cysteine rich glycoproteins that are of importance in proliferation, differentiation, apoptosis, adhesion, migration and cell polarity. The Wnt5a family is involved in intracellular signaling pathways that are either ß-catenin dependent pathways (canonical pathways) or ß catenin independent pathway (non-canonical Wnt signaling pathway). Wnt5a primarily follows the noncanonical pathway. The role of Wnt5a in cancer depends on the tissue type from which the cancer arose, and it can play a tumor suppressing or promoting role. Loss of Wnt5a signaling is correlated to lymphoid malignancies whereas its active signaling plays a role in metastasis and invasion of several cancers.[15]

## 2-Aim

Little is known about the effect of platinum compounds on gene regulation controlled by RNAi mechanisms. This work aims to investigate the combined effect of platinum compounds and RNAi on gene expression. For this purpose Wnt 5a and BRCA1 were selected as downregulation targets for siRNA.

# 3-Materials and methods

## 3-1 Nucleic acid sequences and plasmids used

The sequences were ordered from IBA, BioTAGnology in Göttingen, Germany. The numbers in the nomenclature refer to the nucleotide at which the base pairing starts within the 3'-UTR of Wnt5a protein. The antisense strand of W-siRNA139 was platinated and labeled. In cellular studies, both strands were hybridized prior to transfection into cells.

Table1. siRNA sequences used in this thesis.

| siRNA | Sense/Antisense | Sequence |
|---|---|---|
| W-siRNA33 | Sense | 5'GGACCCGCUUAUUUAUAGATT3' |
| | antisense | 3'TTCCUGGGCGAAUAAAUAUCU5' |
| W-siRNA147 | Sense | 5'GAACUCUGUGGUUUAUUAUTT3' |
| | antisense | 3'TTCUUGAGACACCAAAUAAUA5' |
| W-siRNA139 | Sense | 5'CCAUCUAAGAACUCUGUGGdTdT3' |
| | antisense | 3'dTdTGGUAGAUUCUUGAGACACC5' |
| W-siRNA101 | Sense | 5'CCAAGAAUUGCAACCGGAAdTdT3' |
| | antisense | 3'TdTdGGUUCUUAACGUUGGCCUU5' |
| BRCA1 siRNA | Sense | 5'CAUACAGCUUCAUAAUAUAdTdT3' |
| | antisense | 3'GGUAUGUCGAAGUAUUUAUU5' |

Plasmids used in the Wnt5a system were: pRL-CMV vector from Promega (containing *Renilla* luciferase), and pMIR-REPORT ™ from Ambion (containing firefly luciferase). Bases 1-260 of 3'UTR of Wnt5a were cloned between HindIII and SacI sites downstream to the firefly luciferase gene. The plasmids used in this work can be seen in Figure 3.

## 3-2 Cell lines and cell culture techniques

MCF-7 epithelial adenocarcinoma breast mammary gland cells were obtained from Stina Oredssons group (ATCC number: HTB-22). Cells were maintained in Dulbecco's Modified Eagle Medium (DMEM) supplemented with 10% fetal bovine serum (FBS), 1% L-Glutamine and 1% penicillin/streptomycin. Incubation of the cells was performed in a humidified atmosphere with 5% $CO_2$ at 37 °C. The flasks used for cultivation of MCF-7 cells were either 75 $cm^3$ or 25 $cm^3$ T flasks, or petri dishes depending on the desired experimental setting. The cells were typically passaged twice a week and monitored visually to observe confluency.

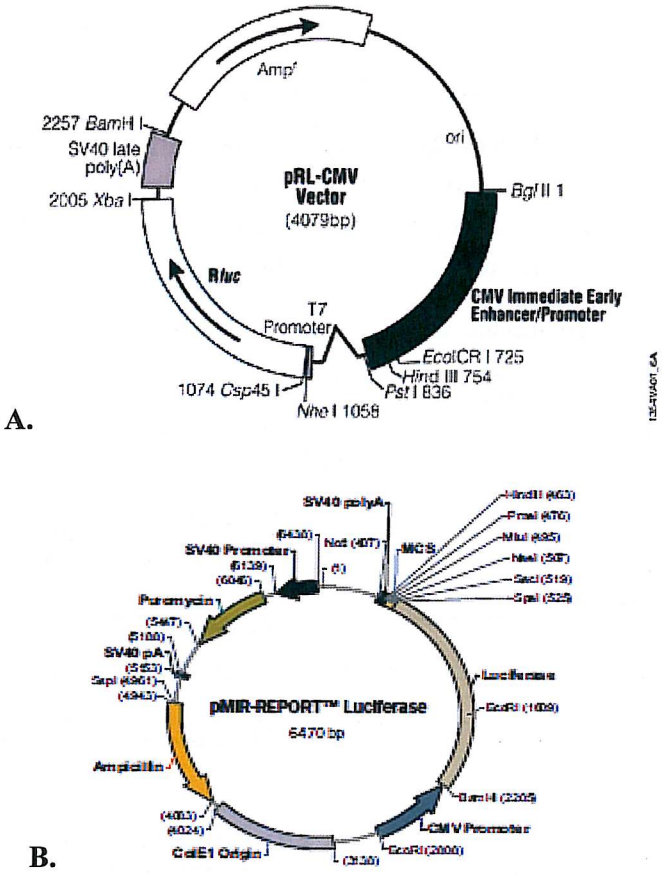


Figure 3. Plasmid map of **A**. pRL-CMV vector containing *Renilla* luciferase and **B**. pMIR-REPORT containing firefly luciferase. Basepairs 1-260 of the Wnt-5a 3'UTR were inserted between the HindIII and SacI site.

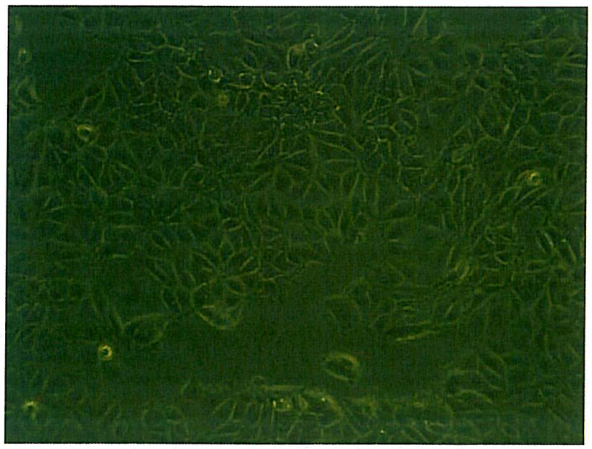

Figure 4. Microscope image of MCF-7 breast adenocarcinoma cells taken by Alak Alshiekh.

## 3-3 Transfection

Lipofectamine™ 2000 (Invitrogen) was used as a transfection reagent. The manufacturer's protocol was followed during transfection. The transfection was performed in different formats depending on the experimental setting used. For Western blotting and protein determination experiments, a 6-well plate format was used and for luminescence measurements, a 24-well plate format was used. For cell vitality assays, a 96-well plate format was used. To get a detectable amount of protein, 300 000 cells were seeded out in each well in a 6-well plate format.

## 3-4 BCA protein determination

The Pierce® BCA protein Assay Kit was used to determine thr total protein content in MCF-7 cell lysates. The manufacturer's protocol was followed, but the amounts were scaled down. The Nanodrop instrument was used for absorbance measurments. The protein determination was performed so that equal amounts of protein could be loaded on the SDS gels.

## 3-5 BRCA1 downregulation

To determine siRNA downregulation capacity, protein levels of BRCA1 were detected by Western blotting. The first approach was to determine the lowest amount of total protein resulting from cell lysis, at wich BRCA1 levels are still detected using Western Blot. For this purpose, the total amount of protein in MCF-7 cell lysates was first determined using BCA protein determination, and then a serial dilution of the cell lysate was loaded on two separate SDS page gels. One of the gels was stained with comassie brilliant blue and the other was blotted on polyvinylidine fluoride (PVDF) membrane. The second approach was to detect endogenous BRCA1 protein level variation after transfection with siRNA targeting a region of the 3'UTR of BRCA1. To detect BRCA1 monoclonal mouse antibody was purchased from Pierce (® BRCA1 prod #MA1-90709 Lot#MG1442643)

In order to determine siRNA effect on endogenous BRCA1 protein production in MCF-7 cells by Western blotting, MCF-7 cells were seeded out in a 6-well plate format at the density of 300 thousand cells per well. Transfection with siRNA QIAGEN ® Hs_BRCA1_15 (HP GenomeWide siRNA) was performed 24 hours after seeding and cell lysis took place either 24 or 44 hours after transfection. The amounts of siRNA used were 5, 25 and 50 picomoles. Cells with no siRNA were used as a negative control.

## 3-6 Cell lysis

For Western blotting experiments, cellular samples were lysed using ProteoJET Mammalian Cell Lysis Reagent in the presence of protease inhibitor cocktail (SIGMA ALDRICH). This lysis method is compatible with the protein determination method used before loading the samples on SDS-PAGE gels for subsequent blotting.

For luciferase assays the samples were lysed using Passive lysis buffer (Promega) provided with the dual glow Luminescence kit. The manufacturer's protocol was followed and the cells were scraped off the plate using pipette tips and the samples were stored at -80 ° C until analysis.

### 3-7 Luminescence measurements and normalization

Luminescence was measured by using a luminometer GU-FM 24 BioOrbit 1250. Signal values were calculated by multiplying the voltage used for obtaining a signal by the height of the signal. The Dual-Luciferase® reporter assay (Promega) was used for detection of both firefly and *renilla* luciferase. Luminescence measurements were performed 42 hours after transfection.

### 3-8 SDS-PAGE

Samples were run on a 3.9% stacking and 8% resolving sodium dodecyl sulfate polyacrylamide gel electrophoresis (SDS-PAGE) gel at 90 volts until the loading dye reached the resolving gel and then 120 volts till the loading dye ran out of the gel. Samples were boiled at 100° C for 3 minutes with 4X loading buffer containing SDS and DTT. The running buffer used was a Tris-glycine SDS buffer. SDS gels were stained with coomassie brilliant blue.

### 3-9 Western blot

The SDS gels were blotted against a (PVDF) membrane at 100 volts for one hour, using a tris glycine SDS transfer buffer. The membrane was blocked by using 5% nonfat dry milk in PBS. The membrane was washed twice with PBS Tween 0.02% and twice with PBS alone. Over night incubation was performed with BRCA1 mouse monoclonal antibody IgG1 (Thermo scientific 1.6 mg/ml) on a shaker in the cold room. After washing, the membrane was incubated with horse radish peroxidase (HRP) conjugated ß-actin IgG1 mouse monoclonal antibody (abcam HS product code 3002101000) for two hours on a shaker in the cold room. A third washing step was done and the membrane was incubated for one hour with HRP conjugated goat antimouse IgG antibody HRP conjugated. Final washing with PBS containing 5% Tween then PBS followed by developing using ECL chemiluminecance reagents with different exposure time depending on the signal strength.

### 3-10 MTT assay

3-(4,5-Dimethylthiazol-2-yl)-2,5-diphenyltetrazolium bromide MTT, a yellow tetrazole, is reduced to purple formazanin living cells can be used to perform a rapid colorimetric assay for cellular growth and survival e.g. in proliferation and cytotoxicity assays. This method is used to determine $IC_{50}$ i.e. the concentration at which the drug reduces the cell survivial to 50% of the initial value.[16]

MCF-7 cells were seeded in a 94 well format (10000 cells per well), in DMEM (antibiotic free medium), incubated for 24 hours (37 °C, 5% $CO_2$ . Different concentrations of cisplatin (1, 10, 25, 50 and100 µM) and oxaliplatin (5, 50, 125, 250 and 500 µM) were then added. The cells

were additionally incubated for 24 hours. The media was removed and the cells were washed with PBS and then removed. MTT was added to the cells, and the plate was rocked for 10 minutes. Finally the cells were incubated for 1 hour at 37°C. MTT was removed and dimethyl sulfoxide (DMSO) was added (100µl per well). The 563 nm absorbance was read on a plate reader.

## 3-11 Purification of nucleic acids by gel electrophoresis and UV shadowing

Polyacrylamide gel electrophoresis was used to purify nucleotides. Non-radiolabeled samples were typically run on thick urea (8M) denaturing gels. Samples were loaded on the pre-run gels with a loading dye consisting of bromophenolblue and xylene cyanol FF. The gels were run on 15 mA voltage for about 5 hours (i.e. the bromophenolblue dye had migrated out of the gel). UV shadowing at 254 nm reveals nucleic bases on a fluorescent silica plate. The visualized nucleotides were excised and ethanol precipitated.

## 3-12 Ethanol precipitation

Gel purified nucleotides were eluted from the gel by keeping the gel pieces in 400 µl sodium acetate (NaOAc) at +4 °C for 24 hours. The liquid containing the eluted nucleotides was transferred to another tube (a second elution step of adding NaOAc is possible for the gel pieces) to which 100 µl of cold 100% ethanol was added and 0.8 µl of glycogen and kept for one hour at -80 °C or overnight at -20 °C. The precipitated nucleotides werepelleted by centrigugation at (13000 rpm). The supernatant was then removed carefully, without disturbing the pellet. A volume of 50 µl cold 70% ethanol was added to the tube and second centrifugation step (13000 rpm for 15 minutes at +4 °C). The pellet was dried in Speed vac and the precipitated nucleotides were solubulized with autoclaved milliQ water.

## 3-13 Nucleic acid concentration determination

To determine the concentration of nucleotides, absorbance was measured with the Nanodrop and the concentration was determined by using Lambert beers law (Equation 1). The extinction coefficient was supplied by the commercial supplier of the sequences (IBA, bio technology, Göttingen Germany).

$$A = \varepsilon \times L \times C \qquad (1)$$

**Equation 1.** Lambert-Beer law, *A:* absorbance, *ε:* extinction coefficient, *C*: concentration.

For radiolabeled nucleotides, the measured radioactivity was used as an indication of concentration after ethanol precipitation. A Geiger counter (Berthold) was used to detect the radio activity as counts per second (CPS).

## 3-14 Oxaliplatin's effect on siRNA efficacy in MCF-7 cells

MCF-7 cells were seeded out at a density of 60000 cells per well. The cells were cotransfected with either a buffer control, W-siRNA-33 or W-siRNA-147 along with *Renilla* control vector and pMIR-luc containing bases (1-260) of the 3'-UTR of Wnt5a. Four hours after to transfection, the media was removed and the cells were washed with 100 µl PBS prior to addition of growth media containing oxaliplatin (in concentrations of 0, 25, 50 or 100 µM). The cells were lysed 42 hours after transfection, and kept at -80 °C till Luciferase measurements were performed. The signals from the siRNA containing samples were normalized against the buffer control at the same concentration of oxaliplatin. Student's T test was used to determine the statistical significance. Experiments were preformed in duplicates at four occasions.

## 3-15 Platination of siRNAs

Platination reactions were preformed at room temperature in the dark, by using 15 equivalents of cisplatin and 25 equivalents of oxalilplatin in non buffered aqueous solution. The reaction mixture was incubated for at least 16 hours.

## 3-16 Digestion of nucleic acids

Enzymatic digestion was performed by using RNase T1 which specifically cleaves 3'end of guanines, and RNaseA which cleaves at pyrimidine phosphates. A serial dilution of RNaseA in a range starting from 1 to $10^{-6}$ units was performed to determine the working range to be used in further experiments.

Chemical cleavage was obtained by alkaline hydrolysis using a 50 mM sodium carbonate buffer pH 9.0 with 1 mM EDTA. The reaction mixture was was incubated at 95 °C for 20 minutes.

## 3-17 Radiolabeling, gel purification and precipitation of oligonucleotides

Radio-labeling of 5'end of oligonucleotides with $^{32}P$ was performed by adding 50 pmole of antisense strand of W-siRNA-139, adenosine 5' triphosphate $\gamma P^{32}$ ATP , T4 Polynucleotide kinase enzyme (T4PNK) 10 units in a 1X PNK reaction buffer (50 mM tris/HCL pH 7.6, 10mM $MgCl_2$, 5 mM DTT, 0.1 mM spermine, 0.1 mM EDTA from Fermentas). The reaction mixture was incubated for one hour at 37 °C. Radiolabeled samples were detected by using a phosphorimmager FLA-3000 image reader (Fujifilm), and images were processed using Multigauge software (ver 3.4).Radiolabeled oligonucleotides were separated on thick denaturing PAGE gels (1 mm) containing 8 M urea when the purpose was to separate different adducts resulting from platination reactions. Cleavage reactions were performed to verify the locations of adducts in the sequence thin 8 M urea PAGE gels (0.5 mm) were used for sequencing and they were run typically for 3 hours.

## 3-18 Thermal melting analysis and van't Hoff's plot

UV melting curves of a nucleic acid are used to monitor a thermally induced order-disorder transition i.e. from duplex to single stranded state. A melting curve is obtained by monitoring the increase in UV absorption vs. temperature profile. Thermal melting curves could be analyzed in order to yield values for van't Hoff transition enthalpy and enthropy ($\Delta H$ and $\Delta S$).[17] The midpoint of the transition is defined as the melting temperature ($T_{m)}$. By plotting the reciprocal of the melting temperature ($1/T_m$) against the natural logarithm of the strand concentration (ln $C_T$), the obtained equation could be used to calculate thermodynamic parameters using (equation 2.) for two self complementary strands.

$$\frac{1}{Tm} = \frac{R\ln CT}{\Delta H} + \frac{(\Delta S° - R\ln 4)}{\Delta H} \qquad (2)$$

**Equation 2.** van't Hoff plot calculation. where $T_m$ denotes the melting temperature, $\Delta H$ the enthalpic contribution, $\Delta S$ the entropic contribution, $R$ gas constant .

For the melting studies of W-siRNA-139 Cary4000 UV-vis spectrophotometer was used. Single strand concentrations of 0.1 μM, 0.5 μM, 1μM, 2μM and 5μM concentration were used for determination of $\Delta H$, $S\Delta$ and $\Delta G$ using Equation 2. The measurments were performed in a 20 mM phosphate buffer (pH 6.3) supplemented with 100 mM sodium chloride.

The first derivative method was used to determine the melting temperature for each concentration. The reciprocal of $T_m$ was then plotted against ln $C_T$ to obtain a van't Hoff's plot and calculate $\Delta H$, $\Delta S$ and $\Delta G$. A Cary WinUV software was used to determine $T_m$ values.

To investigate the effect of platination on thermal stability of w-siRNA-139 the antisense strand was platinated with cisplatin and oxaliplatin. The platination products were gel purified, visualized by UV shadowing and excised. The resulting bands were numbered starting from the upper band with the highest molecular weight, potentially containing newly formed platinum adducts.

## 3-19 Screening the miRNA database (miRBase) for human miRNAs with possible platination sites

The miRNA database (miRBase) [18] was screened for human miRNAs with a possible platination site both in and outside of the seed region to provide a rough guide of possible miRNAs that could be targeted by platinum cancer treatments.

## 3-20 Effect of platination on silencing ability of W- siRNA -101

Efforts to elucidate the effect of seed region platination on silencing ability of siRNA, have been made by Elmroth et. al. The Wnt5a targeting W-siRNA-101 was platinated and gel purified by

Hanna Hedman (private communication). Platination with both cisplatin and oxaliplatin was performed at room temperature in the dark. Gel purified platination products were excised after visualization by UV. The isolated products had either one or two platinum adducts, which were obtained form two platination and purification batches. The nomenclature used in this report can be seen in Table1. Cellular studies were performed in HB2 cells by Hanna Hedman (unpublished data).

Table 2. Nomenclature of W- siRNA -101 adducts used in cellular studies.

| **Nomenclature** | **Explanation** |
|---|---|
| W-siRNA-101 cisPt 2-1 | Contains two cisPt adducts 1$^{st}$ purification batch |
| W-siRNA-101 cisPt 2-2 | Contains two cisPt adducts 2$^{nd}$ purification batch |
| W-siRNA-101 cisPt 1-1 | Contains one cisPt adducts 1$^{st}$ purification batch |
| W-siRNA-101 cisPt 1-2 | Contains one cisPt adducts 2$^{nd}$ purification batch |
| W-siRNA-101 oxPt 2-1 | Contains two oxPt adducts 1$^{st}$ purification batch |
| W-siRNA-101 oxPt 2-1 | Contains two oxPt adducts 2$^{nd}$ purification batch |
| W-siRNA-101 oxPt 1-1 | Contains one oxPt adducts 1$^{st}$ purification batch |
| W-siRNA-101 oxPt 1-2 | Contains one oxPt adducts 2$^{nd}$ purification batch |

# 4-Results and discussion

## 4-1 MTT cell survival assay

Linear regression of the obtained MTT curve in MCF-7 cells yielded LC50 values of 39.50 µM for cisplatin and 227 µM for oxaliplatin.

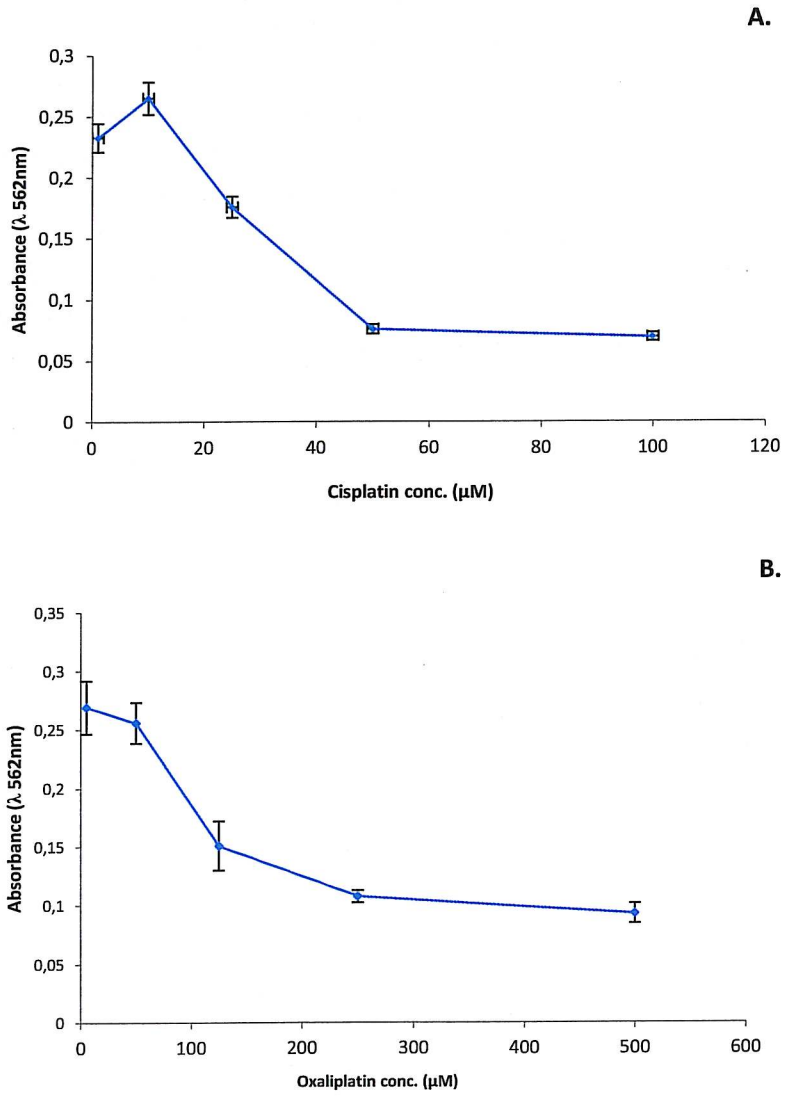


**Figure 5.** MTT assay plot of absorbance at 562 nm against the µM concentration of A. cisplatin and B. oxaliplatin.

## 4-2 Effects of oxaliplatin on siRNA efficacy in MCF-7 cells

This experimental setting aimed to investigate the effects of different concentrations of oxaliplatin on the silencing ability of siRNAs. With increasing platinum concentration cell vitality decreases and thus lower signals are to be expected. For this reason, the luciferase signals were normalized against a buffer control at the same platinum concentration. The down regulation capacity at a 25 μM oxaliplatin concentration was significantly different ($P<0.05$) compared to 0 μM of oxaliplatin for both W-siRNA-33 and W-siRNA-147. Our data suggests that oxaliplatin at a 25 μM concentration slightly decreases the down-regulating capacity W-siRNA-33 and W-siRNA-147 down regulation capacity, however, at a 50 μM concentration the difference was not statistically significant see Figure 6. This experiment serves as a rough simulation to the physiological environment in a cancer cell treated with Platinum. The fact that platinum binds to DNA and other cellular targets complicates the results interpretation. With that in mind, oxaliplatin seems to reduce but not abolish down regulation of studied siRNA sequences. Relative luciferase activity normalized to buffer control in the same conditions increased to 1.7 and 1.8 fold for W-siRNA-33 WsiRNA-147 respectively when oxaliplatin was added at a 25 μM concentration.

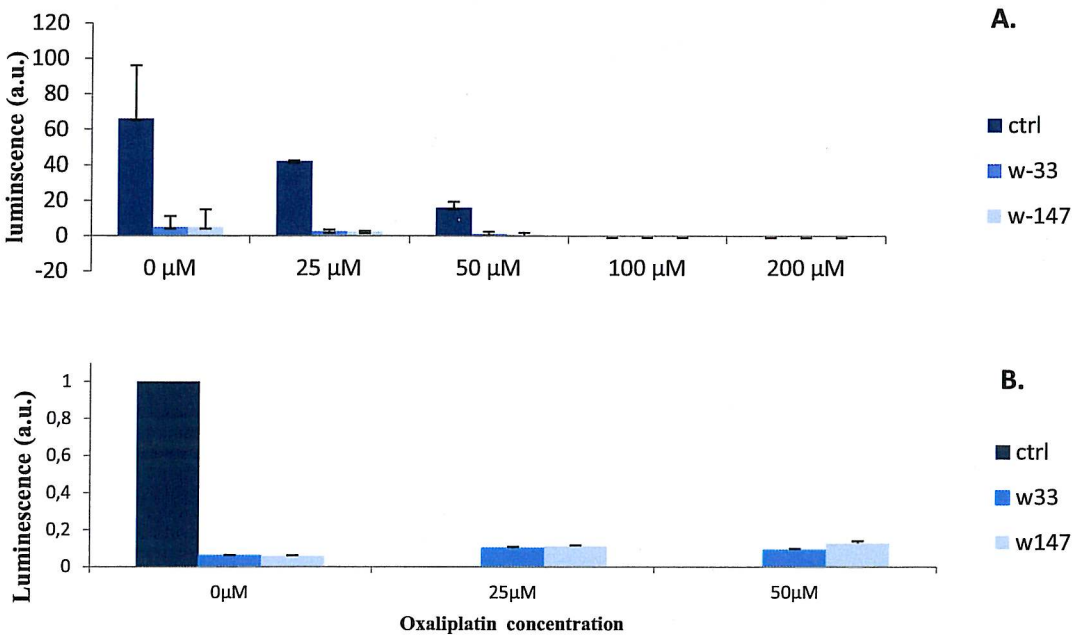


Figure 6. The effect of oxaliplatin on siRNA silencing ability in MCF-7 cells. A. Relative luminescence B. Relative normalized activity is shown. Dark blue bars represent buffer control, medium blue bars represent cells transfected with W-siRNA-33and light blue bars represent cells transfected with W-siRNA-147.* oxaliplatin versus respective buffer-control $P<0.05$, ** $P<0.1$.

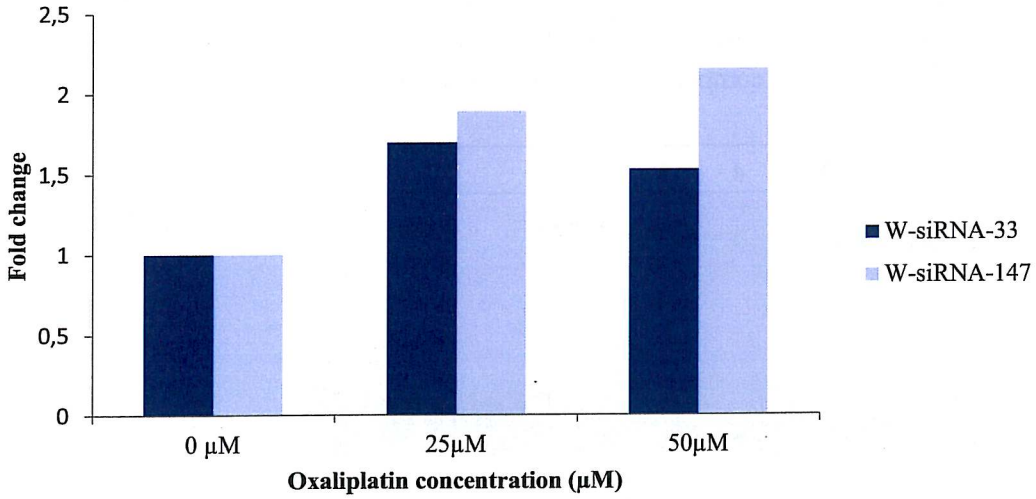


Figure 7. Fold change of relative normalized luciferase protein production compared to production at 0µM oxaliplatin.

## 4-3 BRCA1 level detection by Western blotting

BRCA1 band intensity in ther untransfected cell lysate was notably stronger compared to cells transfected with either buffer or different concentrations of siRNA. The ß-actin signal (used as a loading control) was very strong compared to the BRCA1 signal and it was not possible to get a reproducible signal that could be used to quantify endogenous BRCA1 levels in MCF-7 cell lysates (**Figure 8**). Further optimization is required, before showing siRNA effects on BRCA1 endogenous protein production. Sample size and variability in endogenous BRCA1 protein production were some of the limitations we tried to overcome. Two western blots of samples transfected with increasing concentrations of siRNA, were compared to the buffer negative control and the untransfected cells. (shown in **Figure 9**).

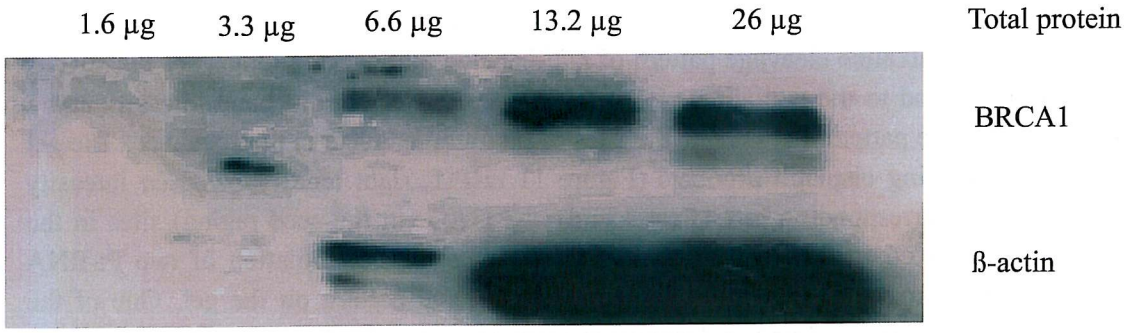


Figure 8. Western blot of a serial dilution of an MCF-7 cell lysate.

## 4-4 BRCA1 downregulation with siRNA

BRCA1 band intensity in the untransfected cell lysate was notably stronger compared to the cells transfected with either buffer or different concentration of siRNA. The ß actin signal used as a loading control was very strong compared to the BRCA1 signal.

A.

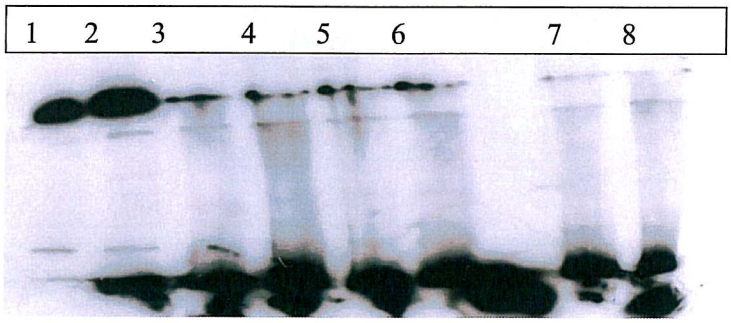


B.

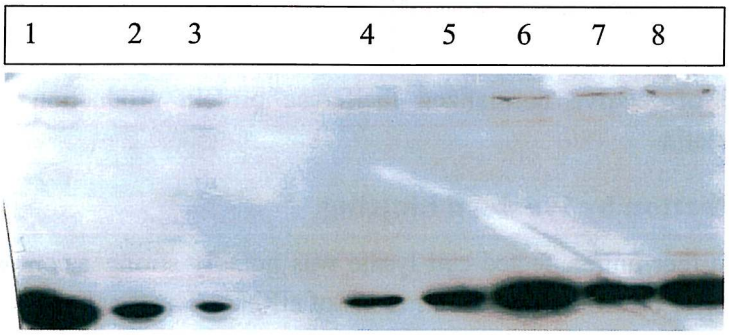


**Figure 9.** A. Western blot of MCF-7 cell lysates. Lanes 1 and 2 represent native cells untreated with lipofectamine and lanes 3 and 4 represent cells transfected with buffer. Lanes 5, 6, 7 and 8 represent cells transfected respectively with either 35, 30, 25 and 5 picomole of BRCA1 siRNA. B. Western blot of an MCF-7 cell lysate. Lanes 1, 2 and 3 represent native cells untreated with lipofectamine and lanes 4, 5, 6, 7 and 8 represent cells transfected respectively with either 5, 25, 30, 35 picomole of BRCA1 siRNA or buffer.

## 4-5 Sequencing of the antisense strand of W- siRNA -139 and determination of platination sites

A comparison of the alkaline cleavage pattern of radiolabeled platination products of the siRNA w-139 antisense strand to the unplatinated control, showed a decrease in band intensity and a change in the cleavage pattern that reveals the sites of platinum adducts in the sequence. The gel purified band containing cisplatin products (Figure 11 cisPt1, right lane) showed an intensity reduction in bands corresponding to GG (at 3'end) and GAG (in the seed region) sites in the sequence as can be seen in Figure 14 lane 11, which suggests the formation of two Pt-RNA adducts that protect from cleavage and changes the migration pattern on the gel. One of the cisplatin bands (cisPt2) showed only a decrease in intensity corresponding to a GAG site which suggests the formation of a single platinum adduct in this product (see Figure 14 lane 10).

Analysis of the oxaliplatin gel purified product (Figure 10 oxPt1, left lane) showed a slight decrease of GG band intensity and no change at GAG position (Figure 13 lane 11), which corresponds to one GAG platinum adduct. The rest of the detected bands showed no change compared to the control suggesting that these bands contian unplatinated species.

**Figure 10.** 5'-end radiolabeled antisense strand of w-siRNA-139.

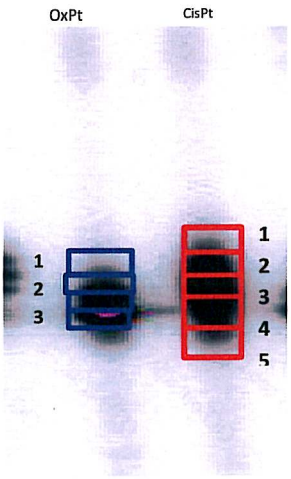


**Figure 11.** Isolated platination products of the 5' labeled antisense strand of W-siRNA-139. The left lane contains oxaliplatin samples, the blue rectangles represent the numbered bands. The middle lane contains the unplatinated control and the right lane is cisplatin treated samples numbered in red rectangles represent isolated bands.

## 4-6 Screening the miRNA database (miRBase) for human miRNAs with possible platination sites

All 1424 human miRNAs annotated in miRBase [18] were screened to look for miRNAs with a tentative platination sites. Known platination sites are GG and GAG sequences. The initial screen showed of miRBase showed that 58.7% of the annotated human miRNAs contain a GG-site in their sequence. We searched for GG-site within in the seed region (nucleotides 2-8 on the antisense strand found that 30% of the sequences annotated in the database (441 miRNAs), have platination sites within the seed region (hits that had a platination at the $8^{th}$ and $9^{th}$ nucleotide were also included). As for GAG sites, it was found that 25% of the annotated miRNAs in miRBase contained GAG site within the sequence and 19% of the annotated miRNAs contain GAG within the seed region (see Figure11 B). The effect of platination agents on endogenous

miRNA, has not been thouroughly investigated. Very little is currently known about the possibe effects of platination on miRNA silencing ability and specificity.The seed region carries the specificity of miRNAs. Our observation is that roughly 30% of the human miRNAs are prone to platination within the seed region .

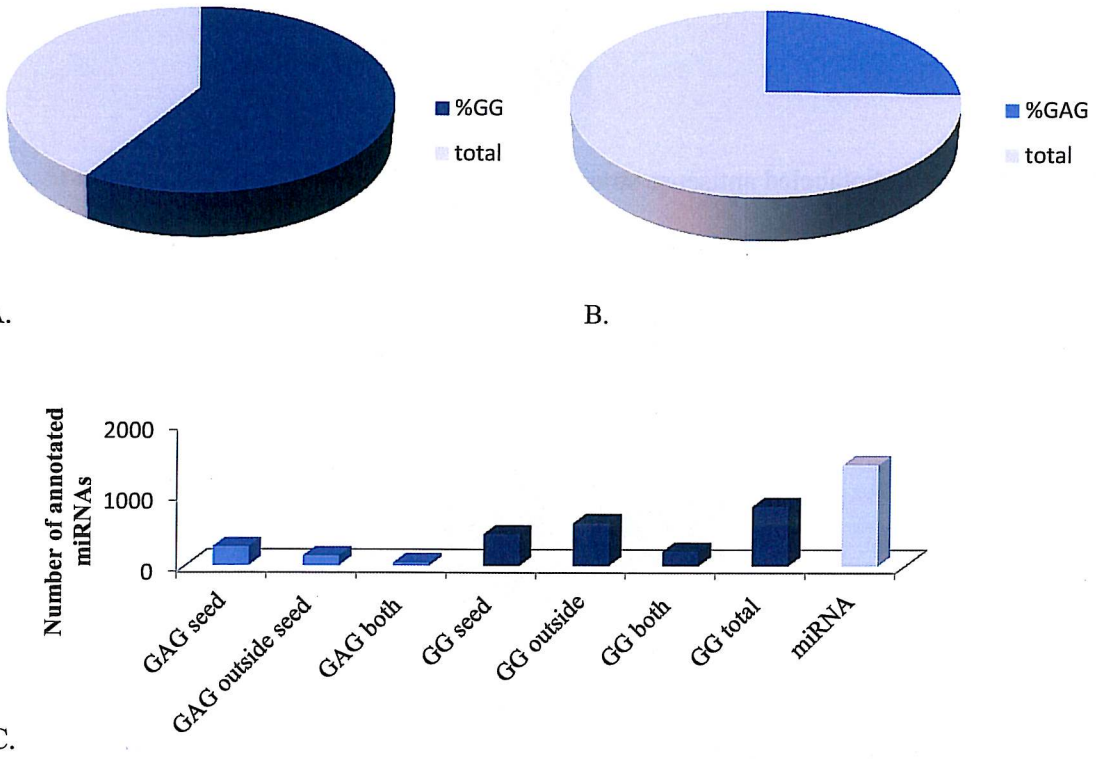


**Figure 12.** A pie chart representation of the percentage of annotated human miRNAs in miRBase, A. miRNAs with a GG platination site within the seed sequence, and B. shows the percentage of miRNAs that have GAG site in the sequence. C. represents number of annotated miRNAs with platination sites .

## 4-7 RNaseA working range determination

The optimal working range of RNaseA that doesn't cause complete degradation of the sequence and yields the expected cleavage pattern, was found to range between $10^{-3}$ and$10^{-5}$ Units. This serves as a guide for further experiments, see **Figure 13**.

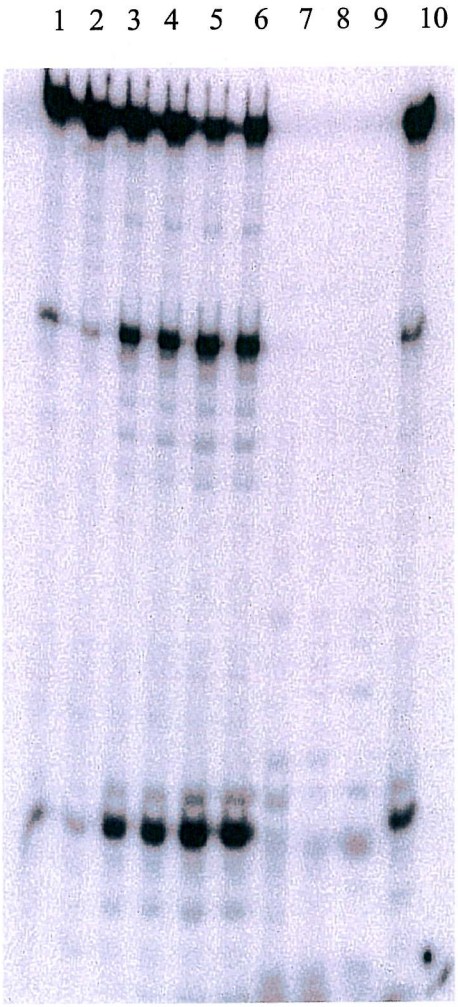


**Figure 13.** RNaseA cleavage of the antisense strand of w-siRNA-139, using a 10-fold serial dilution from a 10 unit stock of RNaseA. Lane 10 contains 10 units of RNaseA, lane 9 contains 1unit, lane 8 contains 0.1 units, lane 7contains 0.01 units, lane6 contains 0.001 units, lane 5 contains $10^{-4}$ units, lane 4 contains $2\times10^{-5}$ units, lane 3 contains $10^{-5}$ units, lane 2 contains $10^{-6}$ units and lane 1 contains $10^{-7}$ units.

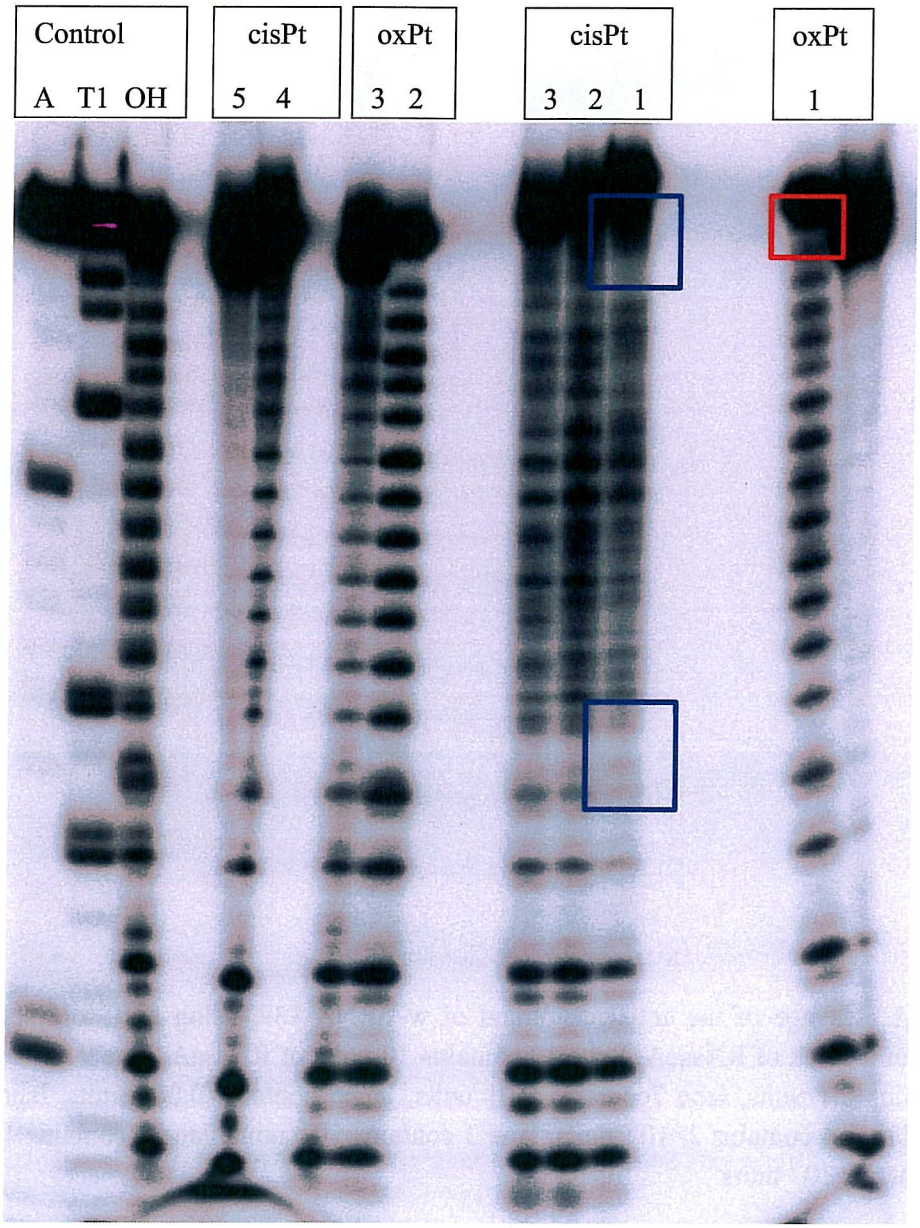


**Figure14.** Cleavage of the anti sense strand of W- siRNA -139. Control lanes contain unplatinated control cleaved by RNAseA in lane (A), T1 enzyme in lane (T1) and by alkaline cleavage in lane (OH). Cisplatin lanes 1-5 contain platination products from Figure 11 cleaved by alkaline cleavage. Lane (1) contains product 1 from cisPt lane in Figure 11, lane (2) contain product 2, lane (3) contains product 3, lane (4) contains product 4 and lane (5) contains product 5. Oxaliplatin lanes represent the alkaline cleavage of oxaliplatin products from Figure 11. Lane (1) contains product 1, lane (2) contians product 2 and lane (3) contains product 3.

## 4-8 Effect of platination on silencing ability of W- siRNA -101

Analysis of relative normalized luciferase activity of siRNA w-101 and its platination products with different number of adducts, shows a significant effect of platination on the silencing ability ($P < 0.025$). The highest effect on downregulating capacity was observed with the species containing two platinum adducts resulting from the oxaliplatin reaction from one of the purification batches (see Table 3). Since both batches are statistically significantly different from each other they were not pooled together. The difference could be attributed to the formation of different products or purification variability. (**Figure 14** and **Table 3**).

The addition of one platinum adduct after reaction with oxaliplatin causes a 1.89 fold change in relative normalized activity compared to non platinated W- siRNA -101. The highest change observed was with the product containing two adducts from both purification batches. The platination product containing two platinum adducts after reaction with cisplatin showed approximately 4.4 fold change in downregulating capacity. We observed that seed region platination did not completely abolish activity of W-siRNA -10,1 it rather attenuated it significantly. This observation requires further investigation to determine what role platinum agents might play in the cellular environment in respect to endogenous miRNAs involved in cancereous processes. From a future perspective it is worth while to investigate the possible interaction between platinum based cancer treatments and the siRNA based therapeutics which are currently being developed.

Table 3. Relative normalized luciferase activity in MCF-7 cells.

| Sample | Average | Fold change | Standard deviation |
|---|---|---|---|
| buffer | 0.15 | - | 0.03 |
| W-siRNA-101 | 0.0064 | - | 0.0010 |
| W-siRNA-101 cisPt2-1 | 0.029 | 4.5 | 0.006 |
| W-siRNA-101 cisPt2-2 | 0.028 | 4.3 | 0.005 |
| W-siRNA-101 oxPt 2-1 | 0.054 | 8.4 | 0.010 |
| W-siRNA-101 oxPt2-2 | 0.019 | 2.9 | 0.007 |
| W-siRNA-101 oxPt-1 | 0.012 | 1.9 | 0.006 |

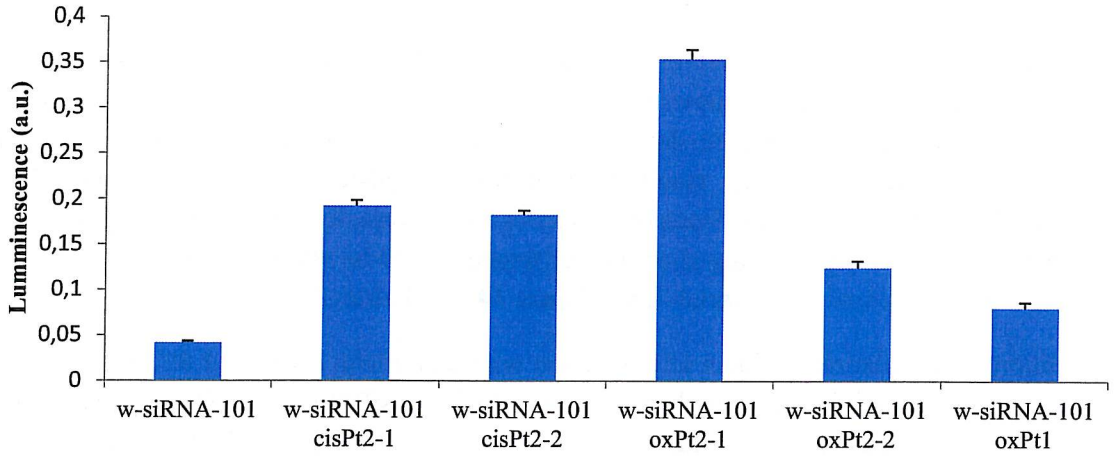


**Figure 15.** Effect of platination on downregulating efficiency of w-siRNA-101.

Relative normalized luciferase activity of W-siRNA-101 and isolated and purified platination products (see Table 2) in MCF-7 cells.

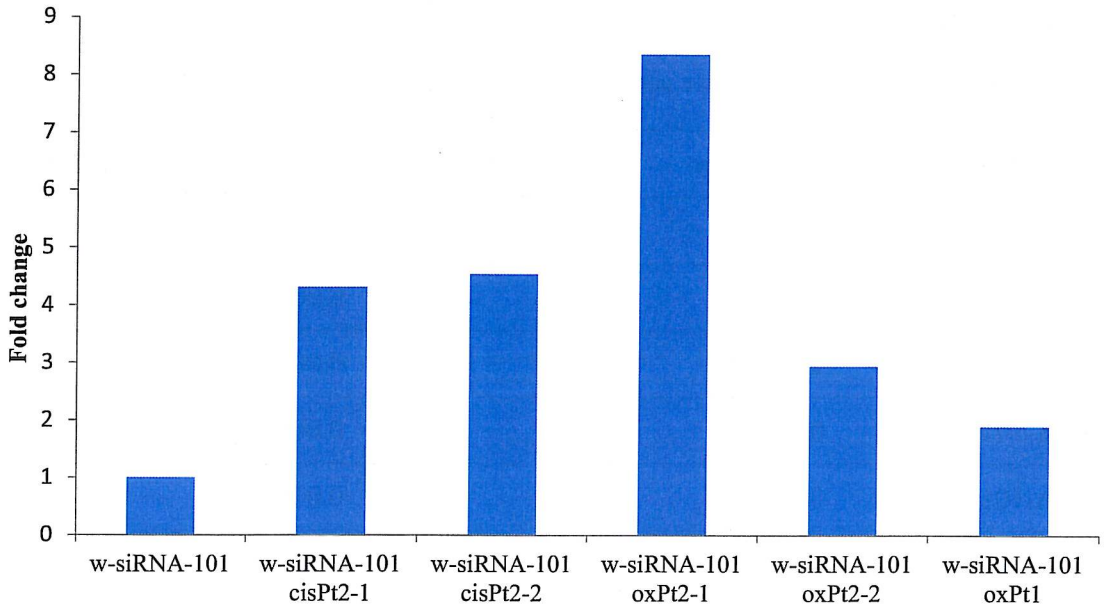


**Figure 16.** Effect of platination on downregulating efficiency of W-siRNA-101Fold change in relative normalized activity in platination products vs. unplatinated control.

## 4-9 Thermal melting studies of W-siRNA-139 and van't Hoff plot analysis

Thermal melting curves obtained for siRNA w-139 are shown in Figure 16, melting temperatures were calculated for each concentration using the first derivative method are shown in Table 4. The reciprocal of $T_m$ in Kelvin vs. the natural logarithm of the total strand concentration was plotted (Figure 18) and a linear regression was done (Equation 3)

$$Y = -0{,}000011\,X + 0{,}002749 \qquad (3)$$

$$R^2 = 0{,}969204$$

$$\frac{1}{Tm} = \frac{RlnCT}{\Delta H} + \frac{(\Delta S° - Rln4)}{\Delta H}$$

Equation 3 Van't Hoff's plot of W-siRNA-139.

By substitution the thermodynamic parameters $\Delta H°$ , $\Delta S°$ and $T\Delta S$ were calculated.

$\Delta H° = 755{,}860\ kJ.K^{-1}.\ mol^{-1}$

$\Delta S° = 2{,}0778\ kJ.K^{-1}.\ mol^{-1}$

$T\Delta S = 619.513$ at 25 °C

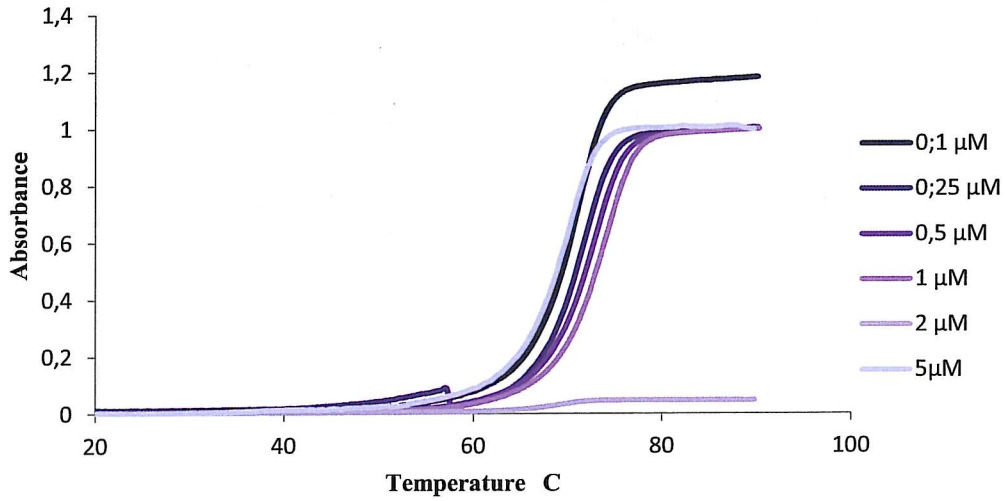


Figure17. Thermal melting curves at increasing concentrations of W-siRNA-139.

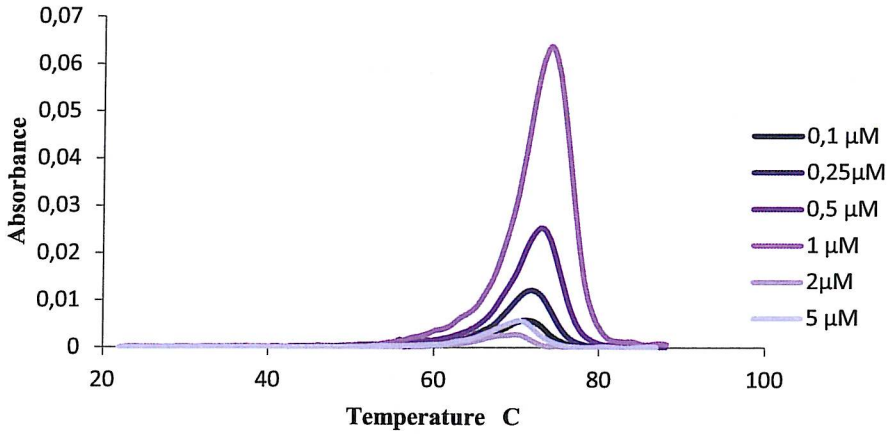


**Figure 18.** First derivative calculated for W-siRNA-139 in concentrations ranging from 0.1 µM to 5 µM.

**Table 4.** Melting temperatures measured at different concentrations of siRNA w-139, were used to obtain van't Hoff's plot.

| Concentration µM | $T_m$ (°C) | $T_m$ (K) | $1/T_m$ ($k^{-1}$) | Total strand conc. (µM) |
|---|---|---|---|---|
| 0.1 | 69.98 | 342.13 | 0.002923 | 0.2 |
| 0.25 | 70.97 | 344.12 | 0.002906 | 0.5 |
| 0.5 | 71 | 344.15 | 0.002906 | 1 |
| 1 | 72 | 345.15 | 0.002897 | 2 |
| 2 | 73.1 | 346.25 | 0.002888 | 4 |
| 5 | 74.15 | 347.3 | 0.002879 | 10 |

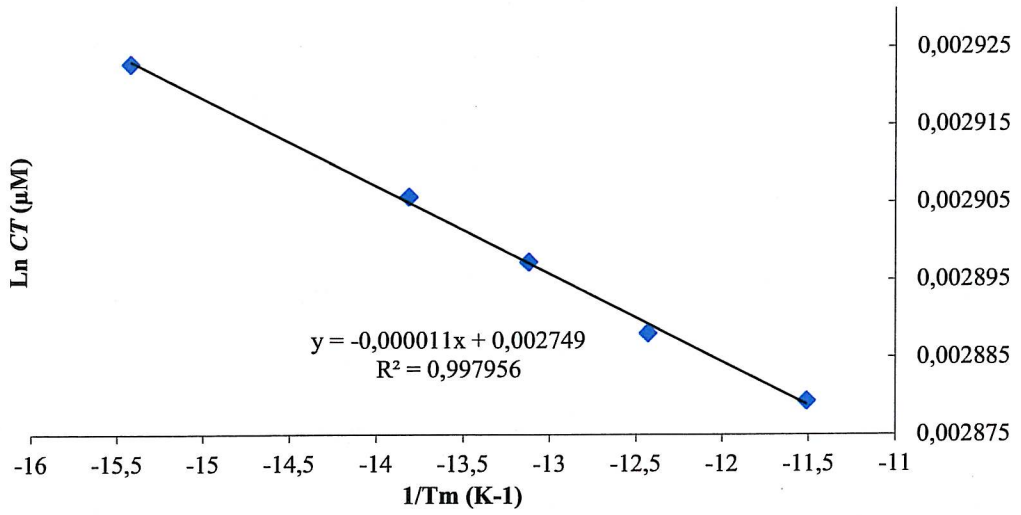


**Figure 19.** van't Hoff plot of W-siRNA-139. Linear regression equation and $R^2$ are shown in the graph.

## 4-10 Platination effect on melting temperature (Tm) and thermodynamic parameters

Comparison of melting temperatures of different platination products to the native unplatinated sequence, gives an estimation of the platinum adducts effect on stability and thermodynamic properties. We observed a decrease in Tm in isolated platination products that migrated slower on the gel and no decrease in *T*m in the products migrating similar to the control. Cisplatin induced a more pronounced decrease in *T*m compared to oxaliplatin. The decreased stability in the cisplatin product (cisPt2) compared to the product (cisPt1) suggests having two Pt adducts in the (cisPt2) one compared to one in (cisPt1). These two different products could in a continuing study be analyzed by mass spectrometry. The observation of two different types of adducts is in line with our previous observation of the sequencing gels of radiolabeled siRNA w139 antisense strand and its platination products, where two platinum adducts (Pt-GG and PtGAG) were detected in the cisplatin product and only one (Pt-GG site) in the second product.

Table 5. Changes in melting temperature induced by platination.

| Duplex | *Tm (°C)* | *Δ Tm (°C)* |
|---|---|---|
| w-siRNA-139 | 69.13 | – |
| w-siRNA-139 cisPt 1 | 60.06 | - 9.07 |
| w-siRNA-139 cisPt 2 | 53.12 | -16.01 |
| w-siRNA-139 oxPt 1 | 61.25 | -7.88 |
| w-siRNA-139 oxPt 2 | 64.30 | -4.88 |

Conditions: $C_{DNA}$ =o.1 μM, CNa+=123 mM, 20 mM phosphate buffer pH 6.3

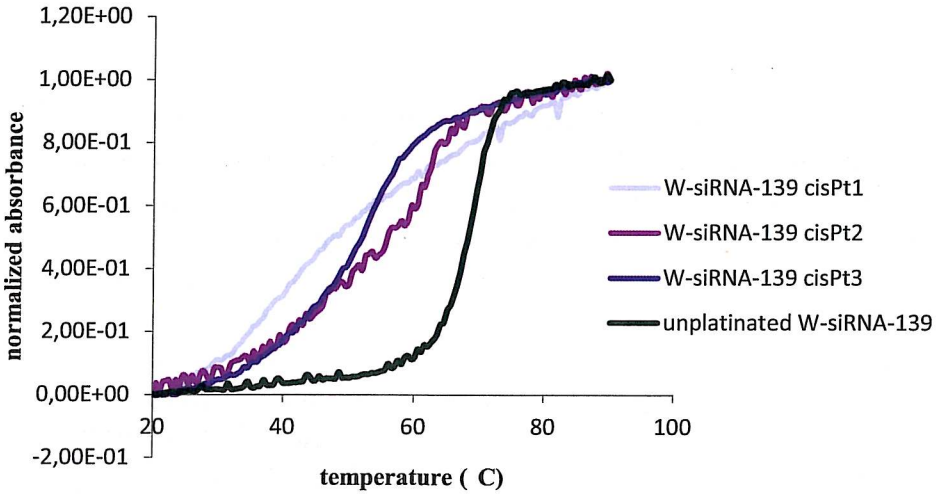


Figure 20. Thermal melting curves of siRNA w-139 and cisplatin platination products (W-siRNA-139 cisPt1, W-siRNA-139 cisPt2 and W-siRNA-139 cisPt3).

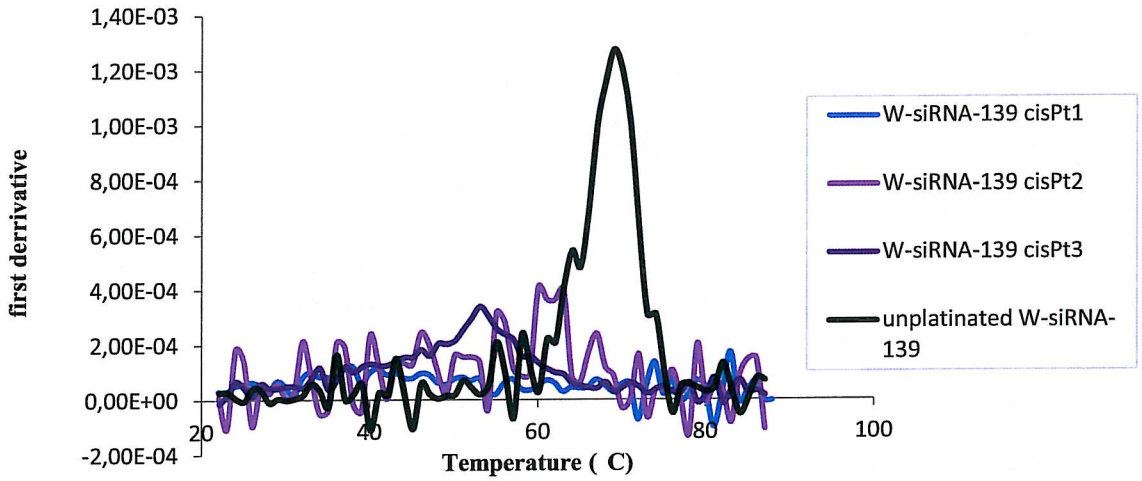


**Figure 21.** First derivative of the thermal melting curves of W-siRNA-139 and cisplatin platination products.

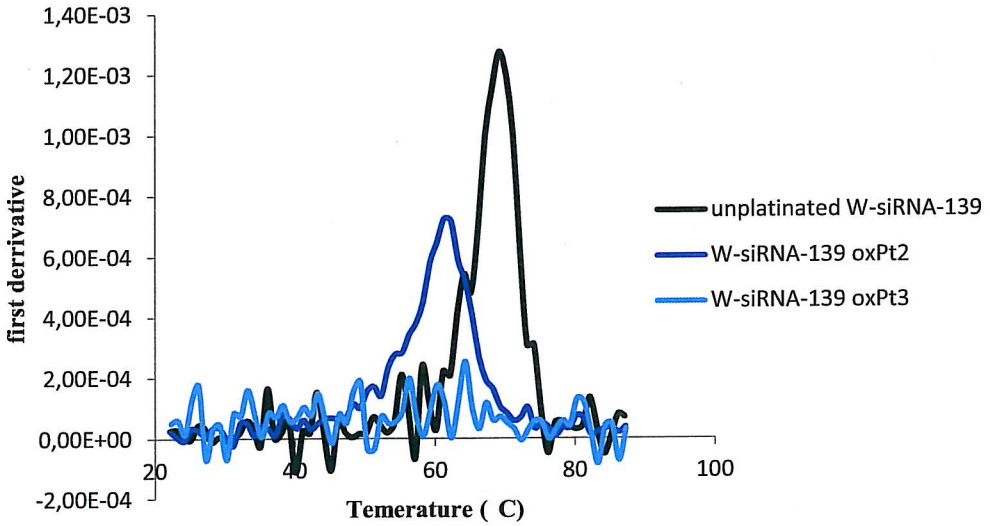


**Figure 22.** First derivative of the thermal melting curves of w-siRNA-139 and oxaliplatin platination products.

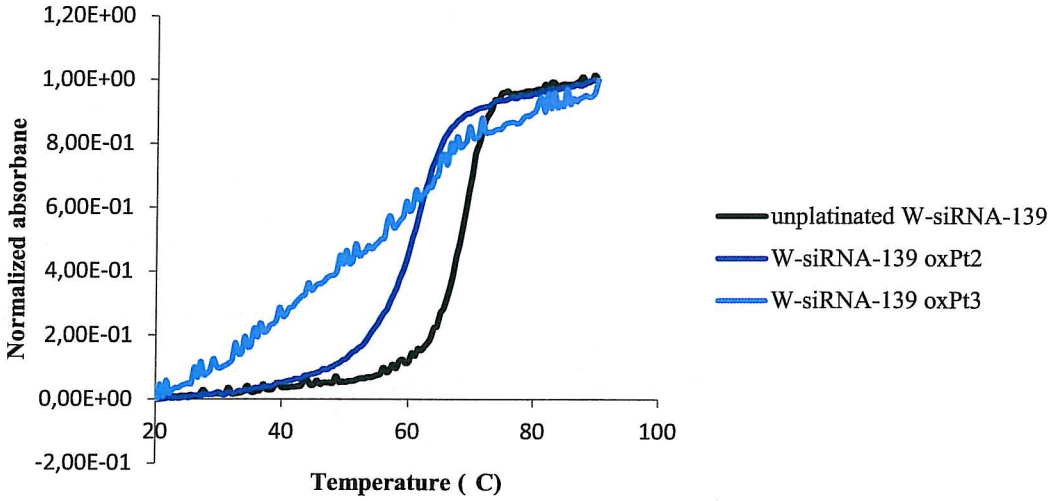


**Figure23.** Thermal melting curve of w- siRNA-139 and oxaliplatin platination products (w-siRNA-139 oxPt2, w-siRNA-139 oxPt2).

## 5-Conclusions

This work tries to shed some light on platinum-RNAi interactions and gain further knowledge about the significance of this interaction both from a thermodynamic and biological point of view. Our preliminary results show that both cisplatin and oxaliplatin affect siRNA in terms of duplex stability and biological activity. Our conclusion is that introduction of Pt-RNA adducts by both oxaliplatin and cisplatin modifies thermodynamic stability of the siRNA duplex and causes a decrease in $T_m$, which shifts the melting curve towards lower temperatures. These adducts also significantly reduce down regulation capacity of active siRNAs, but does not abolish the activity. Addition of oxaliplatin to the growth medium after introducing siRNAs showed a slight change in down regulation as well. In the BRCA1 model system, Western blotting could be a useful tool to quantify siRNA down regulation on the protein level.

## 6-Future perspectives

Future extensions of this work includes studies of the effect of the number and location of formed adducts on duplex stability. Further, an investigaton of the effect of seed region platination would be very interesting to pursue from a biological point of view. Finally, studies improving our understanding of how e.g. platination influences and modifies off target effects may also contribute to improved treatment protocols to be used in the clinic.

## 7-Acknowledgments

I would like to express my gratitude for prof. Dr. Sofi Elmroth for letting me work in the group and letting me step into the RNA and platinum world. All my appreciation to my supervisors Christopher Polonyi, for your patience, guidance and care all through the project, and Hanna Hedman from whom I learned so much. I would also like to thank all the past and current group members for all the cooperation, the efforts and the fun time we have in the lab. A special thanks to Mariana S. Damian for all the advice and support. Personal funding was awareded from Erasmus mundus – Josylen project. My deepest thanks to Nawar, the love of my life and to my family for all the love and support. I would also like to thank all my friends for their support especially Elisabeth for always making me feel at home and Robert for being a real friend all the way. I would also like to thank all the people in the CMPS for making this place such a good working environment and especially the Fika and Lunch crew for all the interesting conversations and all the laughter.

## 8-References


[1] Hanahan, D. and Weinberg, R. Cell **2000,**100, 57–70.

[2] Raymond, E. Faivre, S. Chaney, S. Molecular cancer therapeutics **2002**, 1, 227-235.

[3] Sherman, S.E: Lippard, S.J. Chemical reviews **1987**, 87, 1153-1181.

[4] Rosenberg, H. Van Camp, L. Krigas, T. Nature **1956,** 205, 698-699.

[5] Kelland, L. Nature reviews **2007**, 7 , 573- 584.

[6] Hambley, T.J. Chem. Soc. **2001,** 2711-2718.

[7] Doktycz,M. J. Encyclopedia of life sciences **1997**, 3123.

[8]Mathews, K. van Holde, K.E. Ahren, K.G. Biochemistry third edition 84-118

[9] Fire,A. , Xu, S. Montgomery, M.K. Kostas,S.A. Driver, S.E. Mello, C. Nature **1998,** 391, 806-811.

[10] Mello, C. Conte Jr, D. Nature **2004** , 431, 338-342.

[11] Rana, T.M. Nature reviews, Molecular cell biology **2007,** 8, 23-36.

[12] Garzon, R. Fabbri,M. Cimmino, A. Calin,G.A. and Croce, C.M. Trends in Molecular Medicine **2006**,12 , 580-587

[13] Bumcrot,D. Manoharan,M. Koteliansky,V. & Sah, D.W.Y. Nature chemical biology **2006,** 2, 711-719.

[14] Rosen, E.M. Fan, S. Pestell, R.G. Goldberg, I. D. Journal of cellular physiology, **2003,** 196,19-41.

[15] Nishita,M. Enomoto, M. Yamagata, K. Minami,Y. Trends in cell biology **2010**, 20, 346-354.

[16] Mosmann, T. Journal of lmmunological Methods **1983**, 65 , 55-63.

[17] Markey, L. A. Breslauer, K. J. Biopolymers **1987**, 26, 1601-1618.

[18] http://www.mirbase.org/.

[19] Puglisl, J.D. and Tinoco, I. JR. Absorbance Melting Curves of RNA, characterization of RNAs 304-325.

[20] Markey, L. A. Breslauer, K. J. Biopolymers **1987**, 26, 1601-1618.

# 9-Appendix

## 9-1List of Figures

**Figure 1.** Cisplatin, cis-Pt Cis-diamine dichloride platinum

**Figure 2.** Oxaliplatin, *SP*-4-2-(1*R*-trans)]-(1,2-cyclohexanediamine-*N,N*)[ethandioata-*O,O*]platinum(II).

**Figure 3.** Plasmid map of **A.** pRL-CMV vector containing *Renilla* luciferase and **B.** pMIR-REPORT containing firefly luciferase. Basepairs 1-260 of the Wnt-5a 3'UTR were inserted between the HindIII and SacI site.

**Figure 4.** Microscope image of MCF-7 breast adenocarcinoma cells.

**Figure 5.** MTT assay plot of absorbance at 562 nm against the μM concentration of A. cisplatin and B. oxaliplatin.

**Figure 6.** The effect of oxaliplatin on siRNA silencing ability in MCF-7 cells. A. Relative luminescence B. Relative normalized activity is shown. Dark blue bars represent buffer control, medium blue bars represent cells transfected with W-siRNA-33and light blue bars represent cells transfected with W-siRNA-147.* oxaliplatin versus respective buffer-control $P<0.05$, ** $P<0.1$.

**Figure 7.** Fold change of relative normalized luciferase protein production compared to production at 0μM oxaliplatin.

**Figure 8.** Western blot of a serial dilution of an MCF-7 cell lysate.

**Figure 9.** A. Western blot of MCF-7 cell lysates. Lanes 1 and 2 represent native cells untreated with lipofectamine and lanes 3 and 4 represent cells transfected with buffer . Lanes 5, 6, 7 and 8 represent cells transfected respectively with either 35, 30, 25 and 5 picomole of BRCA1 siRNA.
B. Western blot of an MCF-7 cell lysate. Lanes 1, 2 and 3 represent native cells untreated with lipofectamine and lanes 4, 5, 6, 7 and 8 represent cells transfected respectively with either 5, 25, 30, 35 picomole of BRCA1 siRNA or buffer.

**Figure 10.** 5'-end radiolabeled antisense strand of w-siRNA-139.

**Figure 11.** Isolated platination products of the 5' labeled antisense strand of W-siRNA-139. The left lane contains oxaliplatin samples, the blue rectangles represent the numbered bands. The middle lane contains the unplatinated control and the right lane is cisplatin treated samples numbered in red rectangles represent isolated bands

**Figure 12.** A pie chart representation of the percentage of annotated human miRNAs in miRBase, A. miRNAs with a GG platination site within the seed sequence, and B. shows the

percentage of miRNAs that have GAG site in the sequence. C. represents number of annotated miRNAs with platination sites

**Figure 13.** RNaseA cleavage of the antisense strand of w-siRNA-139, using a 10-fold serial dilution from a 10 unit stock of RNaseA. Lane 10 contains 10 units of RNaseA, lane 9 contains 1unit, lane 8 contains 0.1 units, lane 7contains 0.01 units, lane6 contains 0.001 units, lane 5 contains $10^{-4}$ units, lane 4 contains $2\times10^{-5}$ units, lane 3 contains $10^{-5}$ units, lane 2 contains $10^{-6}$ units and lane 1 contains $10^{-7}$ units.

**Figure14.** Cleavage of the anti sense strand of W- siRNA -139. Control lanes contain unplatinated control cleaved by RNAseA in lane (A), T1 enzyme in lane (T1) and by alkaline cleavage in lane (OH). Cisplatin lanes 1-5 contain platination products from Figure 11 cleaved by alkaline cleavage. Lane (1) contains product 1 from cisPt lane in Figure 11, lane (2) contain product 2, lane (3) contains product 3, lane (4) contains product 4 and lane (5) contains product 5. Oxaliplatin lanes represent the alkaline cleavage of oxaliplatin products from Figure 11. Lane (1) contains product 1, lane (2) contians product 2 and lane (3) contains product 3.

**Figure 15.** Effect of platination on downregulating efficiency of w-siRNA-101.

Relative normalized luciferase activity of W-siRNA-101 and isolated and purified platination products (see Table 2) in MCF-7 cells.

**Figure 16.** Effect of platination on downregulating efficiency of W-siRNA-101

Fold change in relative normalized activity in platination products vs. unplatinated control.

**Figure17.** Thermal melting curves at increasing concentrations of W-siRNA-139

**Figure 18.** First derivative calculated for W-siRNA-139 in concentrations ranging from 0.1 μM to 5 μM.

**Figure 19.** van't Hoff plot of W-siRNA-139. Linear regression equation and $R^2$ are shown in the graph.

**Figure 20.** Thermal melting curves of siRNA w-139 and cisplatin platination products (W-siRNA-139 cisPt1, W-siRNA-139 cisPt2 and W-siRNA-139 cisPt3).

**Figure 21.** First derivative of the thermal melting curves of W-siRNA-139 and cisplatin platination products.

**Figure 22.** First derivative of the thermal melting curves of w-siRNA-139 and oxaliplatin platination products.

**Figure23.** Thermal melting curve of w- siRNA-139 and oxaliplatin platination products (w-siRNA-139 oxPt2, w-siRNA-139 oxPt2).

## 9-2 Table legends

**Table 1**. Sequences used in this thesis.

**Table2.** Nomenclature of siRNA w-139 adducts used in cellular studies.

**Table3.** Relative normalized luciferase activity in MCF-7 cells.

**Table 4.** Melting temperatures measured for different concentrations of siRNA w-139 used to determine van't Hoff's plot.

**Table 5.** Changes in melting temperature induced by platination.

## 9-3 3'UTR sequences

### 3'UTR of BRCA1 mRNA

5'CTGCAGCCAGCCACAGGTACAGAGCCACAGGACCCCAAGAATGAGCTTACAAAGTGGCCTTTCCAG
GCCCTGGGAGCTCCTCTCACTCTTCAGTCCTTCTACTGTCCTGGCTACTAAATATTTTATGTACATCAGC
CTGAAAAGGACTTCTGGCTATGCAAGGGTCCCTTAAAGATTTTCTGCTTGAAGTCTCCCTTGGAAATCT
GCCATGAGCACAAAATTATGGTAATTTTTCACCTGAGAAGATTTTAAAACCATTTAAACGCCACCAAT
TGAGCAAGATGCTGATTCATTATTTATCAGCCCTATTCTTTCTATTCAGGCTGTTGTTGGCTTAGGGCTG
GAAGCACAGAGTGGCTTGGCCTCAAGAGAATAGCTGGTTTCCCTAAGTTTACTTCTCTAAAACCCTGT
GTTCACAAAGGCAGAGAGTCAGACCCTTCAATGGAAGGAGAGTGCTTGGGATCGATTATGTGACTTAA
AGTCAGAATAGTCCTTGGGCAGTTCTCAAATGTTGGAGTGGAACATTGGGGAGGAAATTCTGAGGCAG
GTATTAGAAATGAAAAGGAAACTTGAAACCTGGGCATGGTGGCTCACGCCTGTAATCCCAGCACTTTG
GGAGGCCAAGGTGGGCAGATCACTGGAGGTCAGGAGTTCGAAACCAGCCTGGCCAACATGGTGAAAC
CCCATCTCTACTAAAAATACAGAAATTAGCCGGTCATGGTGGTGGACACCTGTAATCCCAGCTACTCA
GGTGGCTAAGGCAGGAGAATCACTTCAGCCCGGGAGGTGGAGGTTGCAGTGAGCCAAGATCATACCA
CGGCACTCCAGCCTGGGTGACAGTGAGACTGTGGCTCAAAAAAAAAAAAAAAAAAAAGGAAAATGAA
ACTAGAAGAGATTTCTAAAAGTCTGAGATATATTTGCTAGATTTCTAAAGAATGTGTTCTAAAACAGC
AGAAGATTTTCAAGAACCGGTTTCCAAAGACAGTCTTCTAATTCCTCATTAGTAATAAGTAAAATGTTT
ATTGTTGTAGCTCTGGTATATAATCCATTCCTCTTAAAATATAAGACCTCTGGCATGAATATTTCATAT
CTATAAAATGACAGATCCCACCAGGAAGGAAGCTGTTGCTTTCTTTGAGGTGATTTTTTTCCTTTGCTC
CCTGTTGCTGAA**ACCATACAGCTTCATAAATAA**TTTTGCTTGCTGAAGGAAGAAAAAGTGTTTTTCAT
AAACCCATTATCCAGGACTGTTTATAGCTGTTGGAAGGACTAGGTCTTCCCTAGCCCCCCCAGTGTGCA
AGGGCAGTGAAGACTTGATTGTACAAAATACGTTTTGTAAATGTTGCTGTTAACACTGCAAATAAACT
TGGTAGCAAACACTTCAAAAAA AAAAAAAAAAAA 3'

Bold type indicates BRCA1-siRNA target site.

### Base pairs 1-122 of the 3'UTR of Wnt5a

UGGGUGCCACCCAGCACUCAGCCCCGCUCCCAGGACCCGCUUAUUUA
UAGAAAGUACAGUGAUUCUGGUUUUUGGUUUUUAGAAAUAUUUUUU
AUUUUUCCCCAAGAAUUGCAACCGGAACC

Blue box indicates binding of WsiRNA-33 , green box indicates W-siRNA-147 binding site, black box indicates **W-siRNA-139** binding site and red indicates W-siRNA-101 binding site.